

UDC 621.73.011.001.5

DOI: 10.31548/machinery/2.2024.21

Roman Sivak

Doctor of Technical Sciences, Professor
Polissia National University
10008, 7 Staryi Blvd., Zhytomyr, Ukraine
<https://orcid.org/0000-0002-7459-2585>

Volodymyr Kulykivskiy*

PhD in Technical Sciences, Associate Professor
Polissia National University
10008, 7 Staryi Blvd., Zhytomyr, Ukraine
<https://orcid.org/0000-0002-4652-0285>

Vasyl Savchenko

PhD in Technical Sciences, Associate Professor
Polissia National University
10008, 7 Staryi Blvd., Zhytomyr, Ukraine
<https://orcid.org/0000-0002-0921-1424>

Olena Sukmaniuk

PhD in Historical Sciences, Associate Professor
Polissia National University
10008, 7 Staryi Blvd., Zhytomyr, Ukraine
<https://orcid.org/0000-0003-2485-488X>

Viktor Borovskiy

Senior Lecturer
Polissia National University
10008, 7 Staryi Blvd., Zhytomyr, Ukraine
<https://orcid.org/0000-0002-1759-8155>

**Application of resource-saving extrusion technologies
and an integrated approach to assessing the plasticity of metal parts
in agricultural engineering**

Abstract. Among the promising resource-saving technologies to produce parts with improved performance characteristics, the processes of volumetric plastic deformation of products occupy a prominent place. The research relevance is determined by the need to improve the mechanical properties of deformed metal, increase tool life, and produce high precision stamped products with an appropriate level of technological heredity. The study aims to create the required level of strain hardening and damage resistance of deformed metal and products of complex configuration, which will replace expensive steel grades with cheaper ones with similar service characteristics. To calculate the components of the stress tensor under non-monotonic loading, the anisotropic-strengthening body model is used. The study of theoretical and experimental findings suggests that cold combined extrusion methods should be used to manufacture parts with a flange, which can significantly

Article's History: Received: 26.01.2024; Revised: 24.04.2024; Accepted: 29.05.2024.

Suggested Citation:

Sivak, R., Kulykivskiy, V., Savchenko, V., Sukmaniuk, O., & Borovskiy, V. (2024). Application of resource-saving extrusion technologies and an integrated approach to assessing the plasticity of metal parts in agricultural engineering. *Machinery & Energetics*, 15(2), 21-32. doi: 10.31548/machinery/2.2024.21.

*Corresponding author



Copyright © The Author(s). This is an open access article distributed under the terms of the Creative Commons Attribution License 4.0 (<https://creativecommons.org/licenses/by/4.0/>)

increase the boundary dimensions and improve the technological heredity of the product. The study presents a methodology for determining the kinematic characteristics of plastic metal flow using analytical functions obtained from experimental studies of the motion of a continuous medium. The tensor approach was used to create a model of damage accumulation under non-monotonic deformation. The presented complex of calculations can be used to determine the stress state and the amount of the spent plastic deformation resource during non-monotonic volumetric deformation with a sufficiently high accuracy, without preliminary heating of the metal. Based on the information on the stress-strain state and the tensor model of damage accumulation, the ultimate forming of parts with a flange was estimated. The practical value of the research lies in the use of the proposed approaches to solve several technological problems of metal processing by pressure when the material undergoes non-monotonic plastic deformation under conditions of bulk stress

Keywords: cold combined extrusion; non-monotonic deformation; complex loading; metal ductility; three-dimensional stamping

INTRODUCTION

The main focus of machine building development is the study and implementation of the latest technologies based on scientific research. Instead of traditional methods of forming parts by material removal, such as chip peeling, three-dimensional plastic deformation processes are becoming more common. Improvements in engineering technology through the introduction of these processing methods will significantly improve the accuracy and quality of parts. In modern conditions, this is a key factor in ensuring the efficient use of resources (Sivak *et al.*, 2023).

Among the potential processes in the forging and stamping industry, technological operations of volumetric irreversible deformation are necessary. The production of three-dimensional workpieces by stamping, pressing or forging is distinguished by its unique capabilities, variety of types and high efficiency compared to other shaping methods. The development of volumetric deformation technologies indicates a steady increase in the production of precision parts with guaranteed quality, an expansion of the size range and the use of various materials. The results of research on new technologies described by G. Faraji & H. Torabzadeh (2019) show the effectiveness, competitiveness and prospects of plastic-forming processes.

I.S. Aliiev *et al.* (2023) noted that conventional plastic deformation schemes based on the use of two tools – an active moving tool and a fixed fixture – do not meet current requirements and complex technological tasks. Controlling the properties, plastic flow and technological factors requires much more complex force and kinematic effects. The deformation methods developed based on this approach will create innovative processes for producing high-quality products from affordable materials at low cost.

The use of combined plastic processing methods is increasing in the mechanical engineering industry. These shaping methods are characterised by complex loads created by additional kinematic movements of the tool. The resulting force on the workpiece creates a high level of hydrostatic pressure and multi-variable alternating deformation. This gives the product material unique physical and mechanical characteristics that result from the formation of the required level of macrostructure, strain hardening and damage to the plastically processed metal. In many cases, modern

processing methods make it possible to replace expensive steel grades with more economical ones without compromising the performance of the products. According to the results of experimental studies by Y. Beygelzimer *et al.* (2023), the use of combined extrusion leads to a 16-40% reduction in deformation force compared to traditional methods.

The quality of products manufactured by pressure treatment is significantly affected by the stress-strain state of the workpiece during volumetric plastic deformation. According to V. Mykhalevych *et al.* (2023), many factors affect the metal flow and stress-strain state of the workpiece during the forming process. The main ones are the deformation method, tool configuration, product shape, kinematic mode, workpiece material, etc. The properties of a product are formed under the influence of external kinematic and force factors on the workpiece and depend on the dominant mechanical deformation pattern. V. Kukhar *et al.* (2022) determined that kinematic impact can significantly improve the structure of the deformed metal, eliminate stagnant zones, and reduce deformation irregularities.

However, the theoretical methods for solving the problems of metal forming with reliable results remain imperfect and are not adapted to their practical use. This becomes especially evident when the task requires accounting for the volumetric nature of the metal stress state and non-monotonic loading. In studies of modern methods for assessing stresses and ultimate deformations conducted by M. Brünig *et al.* (2023), significant discrepancies between theoretical and experimental results obtained during deformation under non-monotonic loading were noted. This is determined by the imperfect and insufficiently justified physical equations used in these calculations. The structure of the equations should include independent information on the kinematics of the plastic flow of the metal, plasticity assessment, and the relevant mechanical and functional properties of the material.

Thus, the design of combined cold-forming processes based on the development of new methods for calculating the stress-strain state, as well as assessing the deformability of workpieces under non-monotonic loading and the volumetric stress-strain pattern is important for the creation and improvement of metal-forming processes.

Thus, the study aims to create a clear sequence of calculations taking into account the characteristic features of non-monotonic plastic deformation in the processes of cold combined extrusion to obtain the most accurate assessment of the deformability of workpieces.

MATERIALS AND METHODS

In the theory of plasticity, it is extremely difficult to obtain a solution to a system of differential equations that satisfies the boundary conditions for non-monotonic loading. Therefore, the following mathematical model was used to address the effect of non-monotonicity in stress calculations. To obtain the kinematically velocity field for the problems of axisymmetric stationary flow during extrusion (Dou et al., 2023), a method that can be used in the study of steady-state plastic deformation modes of solid bodies was addressed.

The components of the strain rate tensor $\dot{\epsilon}_{ij}$ were determined from equations approximating the curvature of the dividing grid lines in mixed Eulerian-Lagrangian variables (Fernandez et al., 2020):

$$r = f(\psi, z), \quad (1)$$

where ψ – the curvature function of the dividing grid lines.

The components of the stress tensor σ_{ij} for axisymmetric deformation must comply with the differential equilibrium equations (Yu et al., 2022):

$$\frac{\partial \sigma_r}{\partial r} + \frac{\partial \tau_{rz}}{\partial z} + \frac{\sigma_r - \sigma_\phi}{r} = 0; \quad (2)$$

$$\frac{\partial \sigma_z}{\partial z} + \frac{\partial \tau_{rz}}{\partial r} + \frac{\tau_{rz}}{r} = 0. \quad (3)$$

The boundary conditions were taken in an integral form at the boundaries of the elastic and plastic regions G_1 and G_2 (respectively, at the entrance to the matrix and the exit to the cavity):

$$P_n = 2\pi \int_{G_n} r(\sigma_z v_z + \tau_{rz} v_r) dG, \quad (4)$$

where P_n – the force at the boundary G_n , $n = 1, 2$; v_z, v_r are components of the vector of the external normal to G_n , or in the form of homogeneous boundary conditions on a free surface (Reese et al., 2021):

$$\sigma_z v_z + \tau_{rz} v_r = 0; \quad \tau_{rz} v_z + \sigma_r v_r = 0. \quad (5)$$

The magnitude of the loads P_n is known from an experiment or the problem statement. The components of the stress deviator were determined by the following equation:

$$S_{ij} = \frac{2}{3} \sigma_u(e_u) \frac{\dot{\epsilon}_{ij}}{\dot{\epsilon}_u} - \frac{1}{3} \int_0^{e_u} (1 - \beta(e_u^*)) \sigma_u(e_u^*) \phi(e_u^* - e_u^0) \frac{d^2 \epsilon_{ij}}{de_u^{*2}}(e_u^*) de_u^*. \quad (6)$$

Material characteristics $\sigma_p(e_u)$, $\beta(e_u)$ and $\phi(e_u - e_u^0)$ were determined experimentally.

The parameter β which characterises the Bauschinger effect, was determined by the formula:

$$\beta = \frac{\sigma_{0,2}}{\sigma_u(e_u^0)}, \quad (7)$$

where $\sigma_{0,2}$ – the conditional yield strength at compression testing of the sample, primarily stretched to deformation e_u^0 according to the flow curve $\sigma_u(e_u^0)$.

The dependence of β from the e_u was approximated by the formula (Tu et al., 2020):

$$\beta = \beta_m + (1 - \beta_m) \exp(c \cdot e_u). \quad (8)$$

The function ϕ , which addresses the hereditary effect of the deformation process on the current state of the material during plastic deformation, was also determined based on the results of tensile and subsequent compression tests of cylindrical specimens. At the same time, the value of the function was calculated using the formula:

$$\phi(e_u - e_u^0) = \frac{\sigma_p(e_u) - |\sigma_c(e_u)|}{\sigma_p(e_u^0)(1 - \beta(e_u^0))}, \quad (9)$$

where e_u^0 – the accumulated strain, at which the unloading or breakage of the deformation trajectory occurs; $\sigma_p(e_u)$ – stress under monotonic tension; $\sigma_c(e_u)$ – stresses during compression of the specimen up to the strain e_u , pre-tension up to e_u^0 the stress $\sigma_p(e_u^0)$; $\beta(e_u^0)$ – the value of the Bauschinger parameter at $e_u = e_u^0$.

The experimental values ϕ determined by formula (9), were approximated by the dependence:

$$\phi(e_u - e_u^0) = \phi_0 + (1 - \phi_0) \exp(c_1(e_u - e_u^0)^{c_2}), \quad (10)$$

where ϕ_0 is the asymptotic value ϕ obtained experimentally (for steel 10, $\phi_0 = 0.19$).

The coefficients c_1 and c_2 were calculated using the least squares method and the following values were obtained for steel 10: $c_1 = -22.3$; $c_2 = 0.806$.

Figures 1 and 2 show the experimental dependences for the Bauschinger parameter $\beta(e_u)$ and the function $\phi(e_u - e_u^0)$. The model of damage accumulation under non-monotonic loading is based on the hypothesis that damage is described by a second-rank tensor (Lin et al., 2023). The components of this tensor are determined by the mechanics of plastic deformation in a particular technological process, as well as by material functions that describe the physical and mechanical properties of the metal.

Based on the data of S. Reese et al. (2021), a damage tensor ψ_{ij} was introduced, the components of which were defined as follows:

$$\psi_{ij} = \int_0^{e_u^*} F(e_u, \eta, \mu_\sigma) \beta_{ij} de_u, \quad (11)$$

where $F(e_u, \eta, \mu_\sigma)$ – a positive function that describes the reaction of the material to the stress pattern.

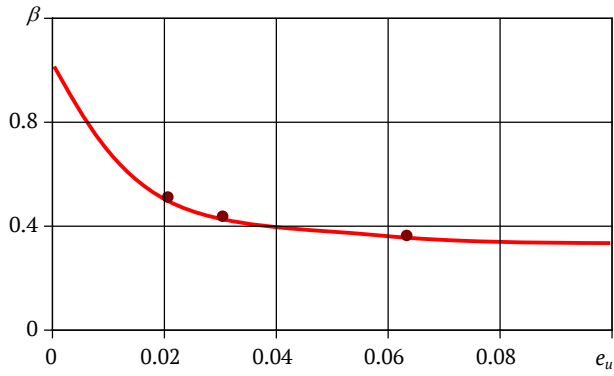


Figure 1. Dependence of the parameter β on e_u
Note: steel 10, approximation $\beta = 0.34 + 0.66 \exp(-62e_u)$
Source: compiled by the authors

The components of the tensor β_{ij} are equal:

$$\beta_{ij} = \sqrt{\frac{2}{3}} \frac{d\varepsilon_{ij}}{de_u} \quad (12)$$

From the correlations of the flow theory:

$$d\varepsilon_{ij} = \frac{3}{2} \frac{de_u}{\sigma_u} S_{ij} \quad (13)$$

According to S. Tu *et al.* (2020):

$$\beta_{ij} = \sqrt{\frac{3}{2}} \frac{S_{ij}}{\sigma_u} = \sqrt{\frac{3}{2}} \frac{S_{ij}}{\sqrt{\frac{3}{2}} \tau} = S_{ij}^0 \quad (14)$$

In solid state physics, there is an analogue of the tensor ψ_{ij} , the dislocation density tensor, which can also be considered as damage. Both tensors are deviators.

When the function of the three invariants of the tensor ψ_{ij} takes on a certain value, this is the beginning of fracture. Exclude from this function the influence of the first invariant, since it is zero, and the third invariant, the fracture condition can be noted as follows:

$$\psi_{ij} \cdot \psi_{ij} = \text{const.} \quad (15)$$

To determine the kinematic characteristics of deformation, the Eulerian and Lagrangian strain tensors were used as the basis (Milenin *et al.*, 2020):

$$E_{ij} = \frac{1}{2} \left(\delta_{ij} - \frac{\partial a_k}{\partial x_i} \cdot \frac{\partial a_k}{\partial x_j} \right); \quad (16)$$

$$L_{ij} = \frac{1}{2} \left(\frac{\partial x_m}{\partial a_i} \cdot \frac{\partial x_m}{\partial a_j} - \delta_{ij} \right), \quad (17)$$

where a is the coordinates of the particle before deformation; x is the coordinates of the particle during deformation, as well as the ratio for determining the deformation rate:

$$\dot{\varepsilon}_{ij} = \frac{1}{2} \left(\frac{\partial v_i}{\partial x_j} + \frac{\partial v_j}{\partial x_i} \right), \quad (18)$$

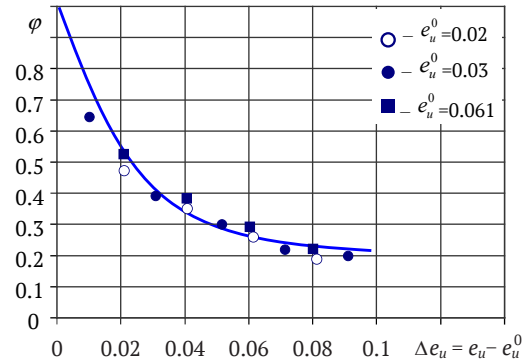


Figure 2. The dependence of a function ϕ on Δe_u
Note: steel 10, approximation $\phi = 0.19 + 0.81 \exp(-22.3 \cdot (e_u - e_u^0)^{0.806})$
Source: compiled by the authors

where v are the components of the velocity of the particles of the deformed body.

The components of the Eulerian strain tensor can be determined if the displacements are specified according to the current coordinates, and the Lagrangian tensor if the position changes are specified depending on the initial coordinates.

RESULTS AND DISCUSSION

It is believed that in the cylindrical coordinate system (r, z) the surface of a matrix can be described by the analytical function $R = R(z)$, which has the corresponding asymptotes: at a $z \rightarrow -\infty, R = R_0 = 1$; at $z \rightarrow \infty, R = R_1$, where R_0 i R_1 – start and end radii (Fig. 3).

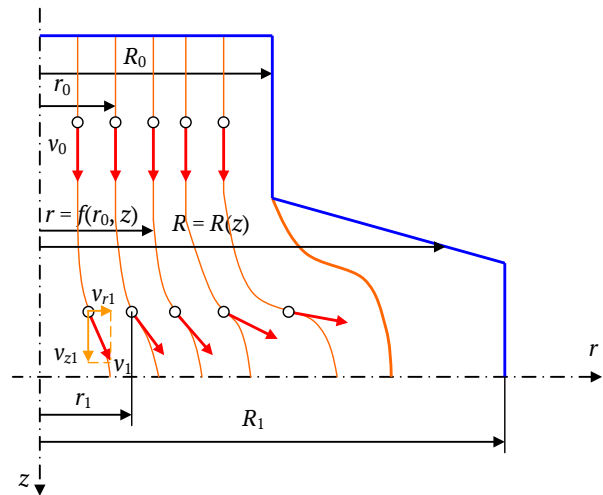


Figure 3. Calculation scheme of curvature of dividing grid lines under axisymmetric deformation, in the general case
Note: r – radius of the contour of a material particle; R – radius of the matrix contour; v_1 – the velocity of a particular particle in the deformation process; v_{r1}, v_{z1} – projections of the velocity of a certain particle in the process of deformation on the axes of the cylindrical coordinate system
Source: compiled by the authors

When constructing the approximations of the dividing grid lines, the following constraints on the functions were set:

☐ in the steady-state stage of motion, all material particles of the deforming metal that have a certain initial co-

ordinate $r_0 = \sqrt{\psi}$ will have the same final coordinate $r_1 = R_1 \cdot r_0$. On the symmetry axis, $r=0$, and the contour, $r=R(z)$. This is possible if equation (1) satisfies the conditions:

$$\lim_{z \rightarrow -\infty} f(\psi, z) = \sqrt{\psi}; \quad \lim_{z \rightarrow \infty} f(\psi, z) = R_1 \sqrt{\psi};$$

$$f(\psi, z) = \begin{cases} 0 & \text{at } \psi = 0; \\ R(z) & \text{at } \psi = 1; \end{cases} \quad (19)$$

☐ on the axis of symmetry, the particle velocities are limited everywhere and, in general, are not equal to zero and the cross-sectional average velocity. That is, at $\psi=0$, the following relations are valid for the components of the velocity vector:

$$v_r(\psi, z) = 0; \quad v_z(\psi, z) < 0; \quad v_z(\psi, z) \neq 0; \quad v_z(\psi, z) \neq 1/R^2(z). \quad (20)$$

At $z \rightarrow \pm\infty$ for all ψ , the components of the velocity vector take the values:

$$\lim_{z \rightarrow -\infty} v_z(\psi, z) = 1; \quad \lim_{z \rightarrow \infty} v_z(\psi, z) = 1/R_1^2, \quad (21)$$

are the components of the strain rate tensor:

$$\dot{\epsilon}_{rz}(\psi, z)|_{\psi=0} = 0; \quad \lim_{z \rightarrow \pm\infty} \dot{\epsilon}_{ij}(\psi, z) = 0. \quad (22)$$

Conditions (1), (19)-(22) imply the following restrictions on the approximation of the curved lines of the dividing grid:

at $\psi=0$:

$$\left| 2f \frac{\partial f}{\partial \psi} \right| < \infty; \quad 2f \frac{\partial f}{\partial \psi} \neq 0;$$

$$2f \frac{\partial f}{\partial \psi} \equiv R^2(z); \quad \frac{\partial f}{\partial z} = 0; \quad 0 < \left| \frac{\partial f}{\partial z} / f \right| < \infty; \quad (23)$$

at $z \rightarrow \pm\infty$:

$$\lim_{z \rightarrow -\infty} \left(2f \frac{\partial f}{\partial \psi} \right) = 1; \quad \lim_{z \rightarrow \infty} \left(2f \frac{\partial f}{\partial \psi} \right) = R_1^2; \quad \lim_{z \rightarrow \infty} \frac{\partial f}{\partial z} = 0. \quad (24)$$

The simplest expression for grid lines that satisfies the requirements (19), (20), (23), (24):

$$f^2(\psi, z) = \psi R^2 + \psi(1 - \psi) \cdot (F_0 + \psi(F_1 - F_0)). \quad (25)$$

Functions F_0 and F_1 depend on the projections onto the axis of the particle velocities along the axis $v_0(z)$ and outline $v_1(z)$:

$$F_0 = \frac{1}{v_0(z)} - R^2(z); \quad F_1 = R^2(z) - \frac{1}{v_1(z)}. \quad (26)$$

Velocity components $v_z(\psi, z)$ the velocity vectors of particles located on the grid line can be determined by the real parameters of the coordinate grid applied to the

meridional section. If the grid spacing along the axis z is constant and equal to Δz_0 , then in their motion the particles move from position 1 to position 2, from position 2 to position 3, and so on, in a period:

$$\Delta t = \frac{\Delta z_0}{v_0} = \Delta z_0. \quad (27)$$

Accordingly, the average speed of particle movement along the z -coordinate from position i to position $i + 1$ equals:

$$v_{zi} = \frac{\Delta z_i}{\Delta z_0}. \quad (28)$$

Velocity determination $v_0 = v_0(0, z)$ and $v_1 = v_1(1, z)$ and expression (28) then in their motion the particles move from position 1 to position 2, from position 2 to position 3, and so on, in a period.

In addition, the velocities $v_z(\psi, z)$ can be determined from experimentally obtained curved grid lines. In each fixed section $z = \text{const}$ (Fig. 3):

$$v_z = \frac{1}{2r} \cdot \frac{\partial \psi}{\partial r} = \frac{\Delta \psi}{\Delta(r^2)} = \frac{r_{0(n+1)}^2 - r_{0(n)}^2}{r_{n+1}^2 - r_n^2}. \quad (29)$$

The experimental information on $v_0(z)$ and $v_1(z)$ was approximated by analytical functions. These functions must satisfy conditions (19), (20), (23), (24). Furthermore, on the symmetry axis:

$$\dot{\epsilon}_{rz} = 0; \quad \dot{\epsilon}_r = \dot{\epsilon}_\phi = -\frac{1}{2} \dot{\epsilon}_z; \quad \dot{\epsilon}_z = \frac{\partial v_0(z)}{\partial z}. \quad (30)$$

Condition (30) implies that at $z = z^*$ which corresponds to the maximum value of $v_0(z)$, all components of the strain rate tensor are equal to zero. This circumstance leads to additional restrictions on the choice of approximation functions for grid lines. Integrating the equilibrium equations along the symmetry axis leads to the result:

$$\sigma_z(0, z) = \sigma_z(0, z_0) + \frac{1}{\sqrt{3}} \int \frac{\partial^2 v_0 / \partial z^2 + 4v_0 (\partial v_0 / \partial z)}{|\partial v_0 / \partial z|} |_{\psi=0}. \quad (31)$$

This means that the equations of the grid lines must also satisfy the following conditions, when $z = z^*$, $\psi = 0$:

$$\frac{\partial^2 v_0}{\partial z^2} + 4v_0 \frac{\partial}{\partial \psi} \left(\frac{1}{2f \frac{\partial f}{\partial \psi}} \right) = 0. \quad (32)$$

Since the integral in expression (31) is taken without complications, at $z = z^*$ and $\psi = 0$ velocity variables $v_0(z)$ and $v_1(z)$ must satisfy the following equality:

$$\frac{\partial^2 v_0}{\partial z^2} + 8v_0^2 \left(2 + \frac{v_0}{v_1} - 3v_0 R^2 \right) = 0. \quad (33)$$

Therefore, the approximations for the functions $v_0(z)$ and $v_1(z)$ can be represented by dependencies:

$$v_0(z) = \frac{1}{R^2(z+c_0)} + \alpha_0 \exp(-\beta_0(z + \gamma_0)^2); \quad (34)$$

$$v_1(z) = \frac{1}{R^2(z+c_1)} + \alpha_1 \exp(-\beta_0(z + \gamma_1)^2). \quad (35)$$

After substituting dependence (29) into expressions (25) and (26), the final formulas for the equations of the

grid lines are obtained, which can be used to calculate all the kinematic characteristics of the plastic flow of metal under steady-state axisymmetric deformation.

The components of the stress deviator are calculated by formula (6), and the stresses under axisymmetric deformation are determined by integrating the differential equilibrium equations (2), and (3) using expression (4). To obtain the tensor model of damage accumulation, the flow theory relations (13) are used, which follow:

$$\frac{d\epsilon_{ij}}{de_u} = \sqrt{\frac{3}{2}} \beta_{ij} = \frac{3}{2} \cdot \frac{S_{ij}}{\sigma_u} \quad (36)$$

Therefore, expression (11), considering formula (9), can be represented as follows:

$$\psi_{ij} = \int_0^{e_u} F(e_u, \eta, \mu_\sigma) S_{ij}^0 de_u \quad (37)$$

or

$$\psi_{ij} = \int_0^{e_u} F(e_u, \eta, \mu_\sigma) S_{ij}^0 f(\alpha_{ij}) de_u, \quad (38)$$

where ψ_{ij} – the main components of the strain tensor; S_{ij}^0 – the main components of the guiding mathematical object that determines the direction of the main axes of the tensor of internal force intensity; $f(\alpha_{ij})$ – a function that determines the effect of load variability; α_{ij} – guiding cosines, which are determined by the angles between the directions of the principal stresses and the coordinate axes associated with the fixed fibres.

To determine the type of a function $F(e_u, \eta, \mu_\sigma)$, a simple load is considered, under which $\beta_{ij}, S_{ij}^0, \eta, \mu_\sigma$ remain constant, therefore:

$$\psi_{ij} = \beta_{ij} \int_0^{e_u} F(e_u, \eta, \mu_\sigma) de_u = \beta_{ij} \phi(e_u, \eta, \mu_\sigma), \quad (39)$$

where $\phi(e_u, \eta, \mu_\sigma) = \int_0^{e_u} F(e_u, \eta, \mu_\sigma) de_u$.

By normalising the sub integral functions in expressions (11), (38) and (39), condition (15) can be brought to the condition accepted in phenomenological theory:

$$\psi_{ij} \cdot \psi_{ij} = 1. \quad (40)$$

From condition (40), considering $\beta_{ij} \cdot \beta_{ij} = 1$, it follows that at $e_u = e_p$ function $\phi(e_u, \eta, \mu_\sigma) = 1$. In addition:

$$\phi(0, \eta, \mu_\sigma) = 0. \quad (41)$$

Satisfying these conditions, it is assumed that:

$$\phi = \sum_{k=1}^m b_k \left(\frac{e_u}{e_p(\eta, \mu_\sigma)} \right)^{n_k}; \quad \sum b_k = 1; \quad n_k > 0, \quad (42)$$

where $e_p(\eta, \mu_\sigma)$ is the surface of ultimate plasticity.

Similarly approximated is the function $f(\alpha_{ij})$, as $S_{ij}^0 \cdot S_{ij}^0 = 1$ (Dai *et al.*, 2022; Chandran & Verleysen, 2024).

As an example, the proposed approach and calculation sequence are used to estimate the plasticity of a metal part with a flange obtained by combined two-stage extrusion. The first stage involves radial extrusion to form a thickening in the centre of the workpiece. Then, in the second stage, the contouring of the thickening is carried out to form a flange. A schematic diagram of the radial extrusion process, followed by the deposition of a cylindrical specimen of steel 10, is shown in Figure 4. The components of the stress deviator for this process are calculated using the formula (6). Hydrostatic stress σ is determined by integrating the differential equilibrium equations, which, under axisymmetric deformation, are of the form (2), (3). At the same time, the integral equilibrium equation is used:

$$P = 2\pi \int_0^R \sigma_z \cdot r \cdot dr, \quad (43)$$

where P is the force determined during the deformation of the body under study; R is the radius of the deformed body.

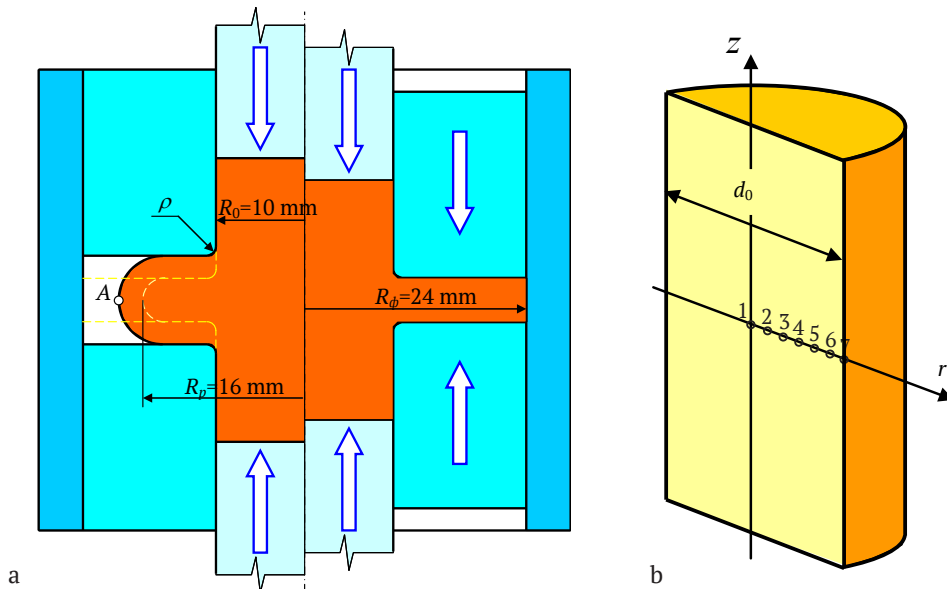


Figure 4. Schematic of a two-stage radial extrusion process followed by contouring of a billet from steel 10 (a) and location of points on the meridional section before deformation (b)

Source: compiled by the authors

Tension σ_r is equal to:

$$\sigma_r = (\sigma_r)_A + \int_r^R \left(\frac{\partial \tau_{rz}}{\partial r} + \frac{S_r - S_\phi}{r} \right) dr, \quad (44)$$

where $(\sigma_r)_A$ is the radial stress at point A (Fig. 4) located on the outer surface of the workpiece.

The axial stress is:

$$\sigma_z = S_z + \sigma_r - S_r. \quad (45)$$

After substituting expressions (44), and (45) into equation (43), we obtain:

$$(\sigma_r)_A = \frac{1}{\pi R^2} \left(P - 2\pi \int_0^R (S_z - S_r + S) r \cdot dr \right), \quad (46)$$

where:

$$S = \int_r^R \left(\frac{\partial \tau_{rz}}{\partial z} + \frac{S_r - S_\phi}{r} \right) dr. \quad (47)$$

The stresses at the remaining points located on the horizontal axis of symmetry of the workpiece were determined by equation (44):

$$(\sigma_r)_i = (\sigma_r)_{i+1} + \int_{r_{i+1}}^{r_i} \left(\frac{\partial \tau_{rz}}{\partial z} + \frac{S_r - S_\phi}{r} \right) dr. \quad (48)$$

Stress σ_z and σ_ϕ are calculated along the radius:

$$(\sigma_z)_i = (\sigma_r)_i - (S_r)_i + (S_z)_i; \quad (49)$$

$$(\sigma_\phi)_i = (\sigma_r)_i - S_r)_i + (S_\phi)_i. \quad (50)$$

The stress along other parallel radii is calculated similarly. Axis stress value σ_z along the vertical lines is

determined by integrating the second differential equilibrium equation (3):

$$(\sigma_z)_{i+1} = (\sigma_z)_i - \int_{z_i}^{z_{i+1}} \left(\frac{\partial \tau_{rz}}{\partial r} + \frac{\tau_{rz}}{r} \right) dz. \quad (51)$$

The stress and strain values obtained in this way are used to display the spatial directions of deformation e_u (η , m_σ), as well as calculations β_i per formula (12) i ψ following the condition (40).

Figure 5 presents the dependences of the components of total stresses, namely σ_z , σ_r and σ_ϕ on the level of deformation e_u at characteristic points (Fig. 4) on the horizontal axis of symmetry of the workpiece (Fig. 4b), at $z = 0$. Analysis of the obtained dependences of the components of total stresses (σ_z , σ_r and σ_ϕ) on the level of deformation e_u (Fig. 5) indicates an accurate correspondence of this theoretical calculation method to the actual deformation process. The dependencies reflect the transition from the first to the second stage of deformation. This is especially pronounced at the points furthest from the vertical axis of symmetry of the workpiece, where the level of non-monotonicity is high. Traditional calculation methods based on flow theory relations do not allow for this result. There is no sharp change like the stress-strain dependence obtained from the flow theory relations at the moment of transition from one extrusion stage to the next. The obtained result indicates the importance of considering the influence of non-monotonic plastic deformation on the patterns of stress field formation under anisotropic strengthening since the reliability of the assessment of the deformability of the workpiece depends on this.

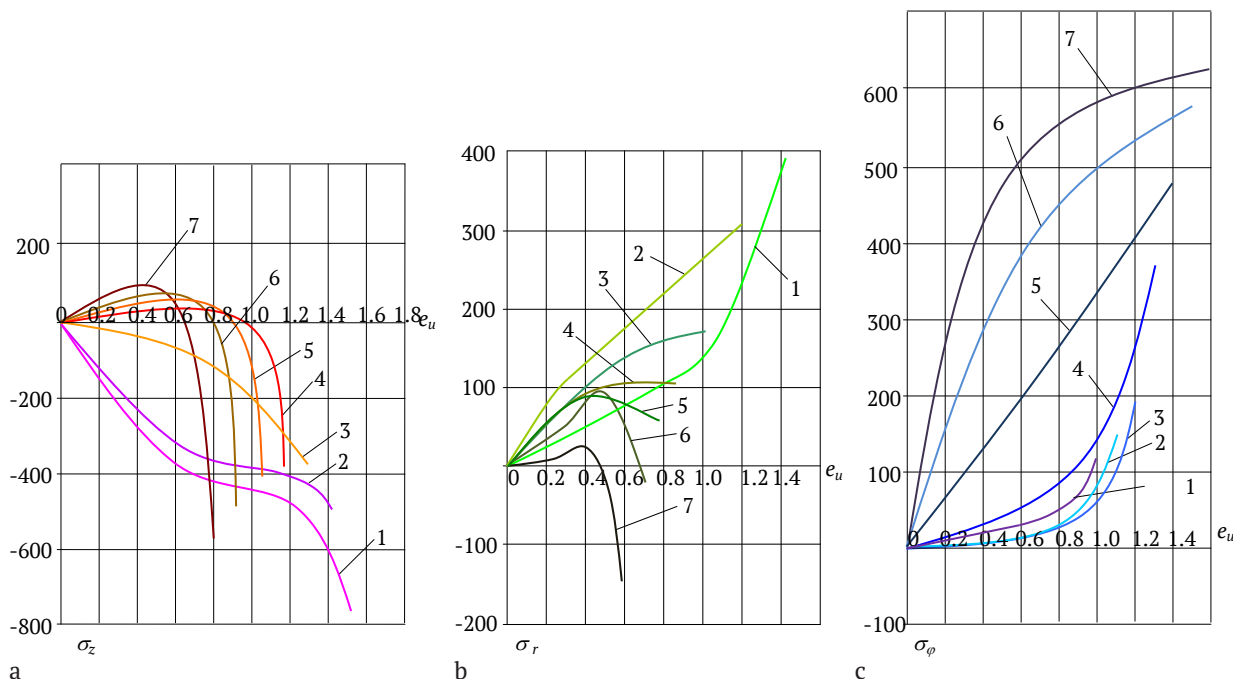


Figure 5. Stress depends on the degree of deformation e_u at characteristic points (1-7)

Note: for $\rho/d_0=0.15$; a) σ_z , b) σ_r , c) σ_ϕ

Source: compiled by the authors

The surface of maximum deformations for steel 10 is approximated by the dependence (Meyer & Menzel, 2021; Sheykin *et al.*, 2021):

$$e_p = (η, μσ) = 0.68 \exp(0.43μσ - 0.71η). \quad (52)$$

The surface of the ultimate deformation of steel 10, as well as the deformation paths of material particles at points 3, 5, and 7 (Fig. 4b), is shown in Figure 6. Position 7 corresponds to point A, which was used in the stress calculation. From the analysis of the nature of the obtained spatial curves and the tendency of their formation in the selected space, it follows that increasing the radius of the die rounding ρ shifts the trajectories to a convenient zone in terms of increasing the plasticity of the metal and therefore improving the deformability of the workpiece. The

experience of producing parts by radial extrusion shows that macro-cracking occurs first of all at the point of the free surface of the flange, on the equatorial axis of symmetry. Contouring reduces the likelihood of fracture in the specified area of the part and provides a flange with a diameter significantly larger than the size of flanges obtained by traditional extrusion methods. In addition, the contact between the free surface of the flange and the matrix creates a region where the metal is in a favourable stress pattern. This further reduces the likelihood of fracture in the danger zone of the part, makes it possible to increase the maximum dimensions and gives the product the necessary technological continuity.

Calculations ψ are shown in Table 1, for a flange with a diameter $d_{max} = 48$ mm (at $d_0 = 20$ mm), depending on the radius of the matrix rounding.

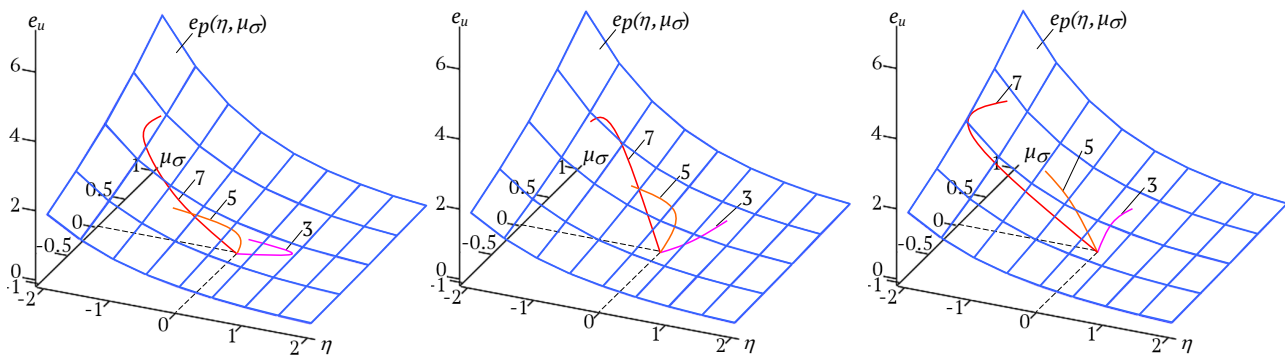


Figure 6. The surface of maximum deformation $e_p(\eta, m_\sigma)$ for steel 10 and the deformation paths of material particles at the points 3, 5, 7

Note: a) $\rho/d_0 = 0.05$; b) $\rho/d_0 = 0.10$; c) $\rho/d_0 = 0.15$

Source: compiled by the authors

Table 1. Results of calculations of the value of the used plasticity resource

The ratio of the rounding radius of the die to the initial diameter of the workpiece, ρ/d_0	Point	The amount of plasticity resource used, ψ
0.05	3	0.48
	5	0.74
	7	0.88
0.10	3	0.39
	5	0.58
	7	0.64
0.15	3	0.36
	5	0.44
	7	0.56

Source: compiled by the authors

The analysis of the results presented in Table 1 shows that increasing the radius of curvature ρ from 1 mm to 2 mm does not affect the amount of plasticity used ψ at the stress point. Only at $\rho = 3$ mm, the value of the used plasticity resource is reduced to $\psi = 0.56$. The deformation of the free surface of the flange during contact with the matrix also has a favourable effect on the amount of plasticity used. If the difference between the values of ψ at points 3 and 5 is large enough, the interval at points 5 and 7 has

been significantly reduced. This fact indicates a reduction in the intensity of damage accumulation in this area of the flange. The radius of curvature of the die is less than 2 mm ($\rho < 2$ mm) leading to an increase in the value of the plasticity resource at the dangerous point, compared to the value ψ at $\rho = 3$ mm. At this value ρ , the flange diameter can reach $d_{max} = 48$ mm ($d_0 = 20$ mm), with no formation of macro cracks on the free surface. Experimental studies have established that the limit value of the flange diameter is

$d_{max} = 52$ mm, for the ratio $\rho/d_0 = 0.15$. The results of the calculations coincide with the experimental results obtained by L. Aliieva *et al.* (2020) and V. Chukhlib *et al.* (2020).

The physical picture of the damage accumulation kinetics under non-monotonic loading has not been studied. Therefore, one of the ways to solve this problem is to apply the hypothesis of the tensor nature of damage accumulation within the phenomenological theory of deformability V. Kukhar *et al.* (2022), which estimates the used plasticity resource under non-monotonic loading. In general, L. Zhou & H. Wen (2019), and M. Brünig *et al.* (2023) used a plasticity diagram to determine the components of the damage tensor. There are no thorough studies devoted to three-dimensional load trajectories under non-monotonic deformation.

The reason for the unsatisfactory accuracy in determining the value of the used plasticity resource under non-monotonic loading is the neglect of strain anisotropy in the assessment of the stress-strain state (Hasemann *et al.*, 2019; Lakshmi *et al.*, 2020). To assess the deformability of future products and ensure the quality of finished parts, information on the deformation history of each material particle in the workpiece volume is required. M.B. Shtern *et al.* (2021) and V. Mykhalevych *et al.* (2023) proposed an original approach to assessing the stress-strain state in the plastic zone, which obtains a sufficiently reliable history of deformation of a part of the material by solving the system of differential equations of the theory of plasticity.

To study the set of stresses and strains both on the outside and inside of the workpieces, one of the most effective methods is the coordinate mesh method, which was studied by G. Faraji & H. Torabzadeh (2019) and I.S. Aliiev *et al.* (2023). The systematic set of steps for macrostructure detection and the microstructural method can also be regarded as ways in which natural grids are used for research (Beygelzimer *et al.*, 2023). The relations for calculating deformations from curved meshes are derived for cases where the original square mesh drawn on the main plane is transformed into a parallelogram after deformation. More general formulas were obtained by V. Kukhar *et al.* (2022) for the case when the initial cell has the shape of a parallelogram, which is especially important when studying the processes of shape change in a stepwise manner. Methods of this type are quite versatile, but the disadvantages include the following: increased labour intensity of measurements, low accuracy of determining small deformations and obtaining averaged results within the cell boundaries. In addition, if the sides of the cell are severely distorted after deformation, this approach leads to large errors.

Along with the direct study of the deformation of a unit cell, the quantification methodology can be based on the step-by-step measurement of the coordinates of points (grid nodes), i.e., determination of the displacement front for a given time interval and subsequent determination of the deformation velocity field. M. Brünig *et al.* (2023) determined that the flow theory relation is used to perform further stress state calculations. When determining the stress state by deformation, it is necessary to address the

relations of the theory of plasticity. The desired stress field must satisfy the equilibrium equations, the plasticity condition, the flow law and the boundary conditions. When determining stresses from kinematics that do not satisfy the boundary conditions during the integration of equilibrium equations, a significant discrepancy between the solutions is observed. According to S. Yoon *et al.* (2022), in some areas, errors can reach hundreds of per cent. The main disadvantage of the considered approaches is that errors in experimental measurements of the curved dividing mesh lead to inaccuracies in the determination of stress deviators. As a result, deviators contain errors that are not always possible to detect and evaluate. The problem in the form of functions that satisfy the equilibrium equations, plasticity condition and boundary conditions can be solved using partial solutions obtained by independent integration of each expression. However, partial solutions can have very significant differences. The approach of W. Dou *et al.* (2023), based on the finite-difference representation of the equilibrium equation, is more reasonable. To accurately satisfy the equilibrium equation at the nodes of the computational grid, a certain relaxation of the requirements for fulfilling the plasticity condition is carried out. The methodology of W. Dou *et al.* (2023) complicates the use of these methods and techniques in areas with complex geometry and cannot be used for the required calculation accuracy. Therefore, when studying the plastic flow of metal, a universal approach is needed to reduce labour intensity and increase the accuracy of calculating kinematic characteristics.

Thus, the proposed complex of calculations is more optimal for determining the stress-strain state and assessing the deformability of workpieces during cold forming, since it addresses the most important indicators of technological processes, which are supplemented by non-monotonic plastic deformation.

CONCLUSIONS

The hypotheses accepted in modern theories of deformability do not always reflect the real nature of damage accumulation under non-monotonic plastic deformation. This leads to an accumulation of errors at each stage of the calculation, from determining the deformation kinematics to estimating the amount of plasticity resource used. A high estimate of the probability of workpiece fracture during metal forming depends on reliable information about the change in the stress-strain state during plastic forming. The known methods for determining the stress-strain state do not always meet modern requirements for assessment accuracy. The value of the used plasticity resource, as one of the indicators of the technological heredity of products, significantly depends on the parameters of an arbitrary technological process. If this process is combined, the determination of this dependence is much more complicated due to the presence of non-monotonic plastic deformation. The obstacle is the reason why the application of many deformability criteria in solving certain technological problems is limited. Therefore, the method of determining

the kinematic characteristics should be the starting point for improving the calculation algorithm. The next step is to determine the components of the stress deviator based on a mathematical model of an anisotropically hardened body that considers the effect of non-monotonic loading. For steel 10, the experimental dependences of the Bauschinger parameter and the hereditary function on the degree of deformation were obtained. The value of the used plasticity resource was estimated using a tensor model. The main difference between the criteria of this model and the known ones is that the surface of the boundary shape change is used instead of the plasticity diagram to approximate the functions describing the mechanical properties of the material.

The proposed sequence of calculating the value of the used plasticity resource was applied to assess the deformability of the workpiece in the process of two-stage cold combined extrusion. As a result, the peculiarities of changes in the value of the used plasticity resource at characteristic points on the horizontal axis of symmetry of the part with a flange were determined. At the same time, the stress state was determined using experimentally derived functions that consider the Bauschinger effect and the hereditary influence of the load history. The components of the strain rate tensor are determined by analytical functions

based on experimental data using Lagrangian and Eulerian coordinates. The boundary strain surface was used as a characteristic reflecting the dependence of plasticity on the stress-strain pattern, and the loading history was set by trajectories in the three-dimensional space of dimensionless stress-strain parameters and accumulated strain. This addresses the effect of non-monotonic plastic deformation under bulk stress conditions. The discrepancy between theoretical and experimental values was assessed by comparing the value of the calculated maximum flange diameter d_{max} and the diameter of the flange with signs of macrocracking. The error between the values was 7-9%. The present work is a continuation of research in the field of plasticity of deformed metal. Further research will be improved by refining the methods of calculating the stress-strain state, quantifying the intensity of damage accumulation, using the theory of dislocations and considering structural transformations in the deformed metal.

ACKNOWLEDGEMENTS

None.

CONFLICT OF INTEREST

None.

REFERENCES

- [1] Aliiev, I.S., Sivak, R.I., Markov, O.E., & Levchenko, V.N. (2023). The evaluation of workpiece deformability for the process of two-stage extrusion of hollow hull. *The International Journal of Advanced Manufacturing Technology*, 129(3-4), 1345-1353. doi: 10.1007/s00170-023-12353-6.
- [2] Aliieva, L., Hrudkina, N., Aliiev, I., Zhibankov, I., & Markov, O. (2020). Effect of the tool geometry on the force mode of the combined radial-direct extrusion with compression. *Eastern-European Journal of Enterprise Technologies*, 2(1(104)), 15-22. doi: 10.15587/1729-4061.2020.198433.
- [3] Beygelzimer, Y., Filippov, A., & Estrin, Y. (2023). 'Turbulent' shear flow of solids under high-pressure torsion. *Philosophical Magazine*, 103(11), 1017-1028. doi: 10.1080/14786435.2023.2180681.
- [4] Brünig, M., Koirala, S., & Gerke, S. (2023). A stress-state-dependent damage criterion for metals with plastic anisotropy. *International Journal of Damage Mechanics*, 32(6), 811-832. doi: 10.1177/10567895231160810.
- [5] Chandran, S., & Verleysen, P. (2024). Non-monotonic plasticity and fracture in DP1000: Stress-state, strain-rate and temperature influence. *International Journal of Mechanical Sciences*, 267, article number 109011. doi: 10.1016/j.ijmecsci.2024.109011.
- [6] Chukhlib, V., Klemeshov, E., Gubskiy, S., Okun, A., & Biba, N. (2020). Theoretical and experimental studies of changes in the workpiece shape during narrow die indentation. In *Advances in design, simulation and manufacturing III* (pp. 361-370). Cham: Springer. doi: 10.1007/978-3-030-50794-7_35.
- [7] Dai, J., Yuan, J., Yang, Z., Zhang, C., Zhang, H., & Yu, S. (2022). Deformation and fracture behavior in TRIP steels under static and dynamic tensile conditions. *Journal of Materials Research and Technology*, 18, 3798-3807. doi: 10.1016/j.jmrt.2022.04.050.
- [8] Dou, W., Xu, Z., Han, Y., & Huang, F. (2023). A ductile fracture model incorporating stress state effect. *International Journal of Mechanical Sciences*, 241, article number 107965. doi: 10.1016/j.ijmecsci.2022.107965.
- [9] Faraji, G., & Torabzadeh, H. (2019). An overview on the continuous severe plastic deformation methods. *Materials Transactions*, 60(7), 1316-1330. doi: 10.2320/matertrans.MF201905.
- [10] Fernandez, F., Puso, M., Solberg, J., & Tortorelli, D. (2020). Topology optimization of multiple deformable bodies in contact with large deformations. *Computer Methods in Applied Mechanics and Engineering*, 371, article number 113288. doi: 10.1016/j.cma.2020.113288.
- [11] Hasemann, G., Müller, C., Grüner, D., Wessel, E., & Krüger, M. (2019). Room temperature plastic deformability in V-rich V-Si-B alloys. *Acta Materialia*, 175, 140-147. doi: 10.1016/j.actamat.2019.06.007.
- [12] Kukhar, V., Povazhnyi, O., & Grushko, O. (2022). Analysis of CuZn5 tube buckling during producing of the crossover bend for metallurgical unit. *Advanced Manufacturing Processes IV* (pp. 444-454). Cham: Springer. doi: 10.1007/978-3-031-16651-8_42.

- [13] Lakshmi, S., Matvijchuk, V., Rubanenko, O., & Branitskyi, Y. (2020). Justification and development of methods building curves boundary deformation of metals. *Materials Today: Proceedings*, 38(1-3), 3337-3344. doi: [10.1016/j.matpr.2020.10.243](https://doi.org/10.1016/j.matpr.2020.10.243).
- [14] Lin, L., Peng, W., Titov, V., Oleksandr, M., Wu, X., & Li, H. (2023). Interface phenomena and bonding mechanism in the new method of cross wedge rolling bimetallic shaft. *Journal of Materials Research and Technology*, 24, 1132-1149. doi: [10.1016/j.jmrt.2023.03.049](https://doi.org/10.1016/j.jmrt.2023.03.049).
- [15] Meyer, K., & Menzel, A. (2021). A distortional hardening model for finite plasticity. *International Journal of Solids and Structures*, 232, article number 111055. doi: [10.1016/j.ijsolstr.2021.111055](https://doi.org/10.1016/j.ijsolstr.2021.111055).
- [16] Milenin, A., Furushima, T., Du, P., & Pidvysots'kyi, V. (2020). Improving the workability of materials during the dieless drawing processes by multi-pass incremental deformation. *Archives of Civil and Mechanical Engineering*, 20(3), article number 86. doi: [10.1007/s43452-020-00092-4](https://doi.org/10.1007/s43452-020-00092-4).
- [17] Mykhalevych, V., Dobraniuk, Y., Matviichuk, V., Kraievskyi, V., Tiutiunyk O., Smailova, S., & Kozbakova, A. (2023). A comparative study of various models of equivalent plastic strain to fracture. *Informatics, Control, Measurement in Economy and Environmental Protection*, 13(1), 64-70. doi: [10.35784/iapgos.3496](https://doi.org/10.35784/iapgos.3496).
- [18] Reese, S., Brepols, T., Fassin, M., Poggenpohl, L., & Wulfinghoff, S. (2021). Using structural tensors for inelastic material modeling in the finite strain regime – A novel approach to anisotropic damage. *Journal of the Mechanics and Physics of Solids*, 146, article number 104174. doi: [10.1016/j.jmps.2020.104174](https://doi.org/10.1016/j.jmps.2020.104174).
- [19] Sheykin, S.Ye., Melnichenko, V.V., Studenets, S.F., Rostotskyi, I.Yu., Iefrosinin, D.V., Melnichenko, Ya.V., & Grushko, O.V. (2021). On the contact interaction between hard-alloy deforming broaches and a workpiece during the shaping of grooves in the holes of tubular products. *Journal of Superhard Materials*, 43, 222-230. doi: [10.3103/S1063457621030096](https://doi.org/10.3103/S1063457621030096).
- [20] Shtern, M.B., Mikhailov, O.V., & Mikhailov, A.O. (2021). Generalized continuum model of plasticity of powder and porous materials. *Powder Metallurgy and Metal Ceramics*, 60, 20-34. doi: [10.1007/s11106-021-00211-7](https://doi.org/10.1007/s11106-021-00211-7).
- [21] Sivak, R., Kulykivskyi, V., Savchenko, V., Minenko, S., & Borovskyi, V. (2023). Determination of porosity functions in the pressure treatment of iron-based powder materials in agricultural engineering. *Scientific Horizons*, 26(3), 124-134. doi: [10.48077/scihor3.2023.124](https://doi.org/10.48077/scihor3.2023.124).
- [22] Tu, S., Ren, X., He, J., & Zhang, Z. (2020). Stress-strain curves of metallic materials and post-necking strain hardening characterization: A review. *Fatigue & Fracture of Engineering Materials & Structures*, 43(1), 3-19. doi: [10.1111/ffe.13134](https://doi.org/10.1111/ffe.13134).
- [23] Yoon, S.-Y., Barlat, F., Lee, S.-Y., Kim, J.-H., Wi, M.-S., & Kim, D.-J. (2022). Finite element implementation of hydrostatic pressure-sensitive plasticity and its application to distortional hardening model and sheet metal forming simulations. *Journal of Materials Processing Technology*, 302, article number 117494. doi: [10.1016/j.jmatprotec.2022.117494](https://doi.org/10.1016/j.jmatprotec.2022.117494).
- [24] Yu, R., Li, X., Yue, Z., Li, A., Zhao, Z., Wang, X., Zhou, H., & Lu, T.J. (2022). Stress state sensitivity for plastic flow and ductile fracture of L907A low-alloy marine steel: From tension to shear. *Materials Science and Engineering: A*, 835, article number 142689. doi: [10.1016/j.msea.2022.142689](https://doi.org/10.1016/j.msea.2022.142689).
- [25] Zhou, L., & Wen, H. (2019). A new dynamic plasticity and failure model for metals. *Metals*, 9(8), article number 905. doi: [10.3390/met9080905](https://doi.org/10.3390/met9080905).

Роман Сивак

Доктор технічних наук, професор
Поліський національний університет
10008, б-р Старий, 7, м. Житомир, Україна
<https://orcid.org/0000-0002-7459-2585>

Володимир Куликівський

Кандидат технічних наук, доцент
Поліський національний університет
10008, б-р Старий, 7, м. Житомир, Україна
<https://orcid.org/0000-0002-4652-0285>

Василь Савченко

Кандидат технічних наук, доцент
Поліський національний університет
10008, б-р Старий, 7, м. Житомир, Україна
<https://orcid.org/0000-0002-0921-1424>

Олена Сукманюк

Кандидат історичних наук, доцент
Поліський національний університет
10008, б-р Старий, 7, м. Житомир, Україна
<https://orcid.org/0000-0003-2485-488X>

Віктор Боровський

Старший викладач
Поліський національний університет
10008, б-р Старий, 7, м. Житомир, Україна
<https://orcid.org/0000-0002-1759-8155>

Застосування ресурсозберігаючих технологій видавлювання і комплексного підходу оцінки пластичності металу деталей в агроінженерії

Анотація. Серед перспективних ресурсозберігаючих технологій виробництва деталей, з покращеними експлуатаційними характеристиками, чільне місце займають процеси об'ємного пластичного деформування виробів. Актуальність досліджуваної теми обумовлена необхідністю підвищення показників механічних властивостей деформованого металу, збільшення стійкості інструменту, отримання високоточних штампованих виробів із належним рівнем технологічної спадковості. Метою дослідження є створення необхідного рівня деформаційного зміцнення та пошкодженості деформованого металу, виробів складної конфігурації, що дозволить замінити дорогі марки сталей більш дешевими, із аналогічними службовими характеристиками. Для розрахунку компонентів тензора напружень, при немонотонному навантаженні, використана модель анізотропно-зміцнюваного тіла. На підставі теоретичних та експериментальних надбань запропоновано, для виготовлення деталей з фланцем, застосовувати способи холодного комбінованого видавлювання, які дозволяють значно збільшити граничні розміри і покращити показники технологічної спадковості виробу. В статті представлена методика визначення кінематичних характеристик пластичної течії металу аналітичними функціями, отриманими на основі експериментальних досліджень руху суцільного середовища. Тензорний підхід дозволив створити модель накопичення пошкоджень при немонотонній деформації. Представлений комплекс обчислень дозволяє достовірно і з досить високою точністю визначити напружений стан, величину витраченого ресурсу пластичної формозміни під час немонотонного об'ємного деформування, без попереднього підігріву металу. На основі інформації про напружено-деформований стан і тензорної моделі накопичення пошкоджень здійснена оцінка граничного формоутворення деталей з фланцем. Практична цінність досліджень полягає у використанні запропонованих підходів для розв'язання низки технологічних задач обробки металів тиском, коли матеріал зазнає немонотонного пластичного деформування в умовах об'ємного напруженого стану

Ключові слова: холодне комбіноване видавлювання; немонотонна деформація; складне навантаження; пластичність металу; об'ємне штампування